The Effect of Elasto-Plastic Properties of Materials on their Formability by Flow Forming

Olga I. Bylya[a], Timur Khismatullin[a], Paul Blackwell[b*] and Rudolf A. Vasin[c]

[a] *Advanced Forming Research Centre, University of Strathclyde, 85 Inchinnan Drive, Inchinnan, Renfrew PA4 9LJ, United Kingdom*

[b] *Mechanical & Aerospace Engineering, University of Strathclyde, James Weir Building, 75 Montrose Street, G1 1XJ*

[c] *Institute of Mechanics, Lomonosov Moscow State University, 2 Michurinsky Prospect, Moscow, Russia*

Abstract

FEA process modelling, which has seen plenty of development in recent decades, has significantly simplified and broadened our capabilities for designing and optimising metal forming processes. It has become relatively easy to find the stress-strain state at any point and instant in the process, analyse the kinematics of metal flow or test different fracture criteria. However, it is frequently the case that all this information cannot compensate for the lack of a fundamental understanding of the process. Flow forming is a case in point. Although much research has been carried out since the 1960's and has resulted in considerable industrial experience, still many aspects remain as "know how" and many basic questions do not have exact answers. This work reported herein is focused on the role of the elasto-plastic properties of a material with respect to its use in flow forming. Can the flow formability of a material be assessed using data from a uniaxial tensile test? If there exists the possibility of tailoring mechanical properties by heat treatment, what should be prioritised?

Keywords: Flow forming, finite element (FE) modelling, heat treatment, complex loading.

* Corresponding author. Tel.: +44 (0) 141 574 5086. E-mail: paul.blackwell@strath.ac.uk

1. Introduction

Flow forming (or tube spinning) is one of the incremental bulk metal forming processes, used for the manufacturing of tubular parts. It is often carried out at room temperature. Although it benefits from the advantages of its incremental nature, flow forming is quite a difficult process to optimise. Plewinski and Denger (2009) pointed out that the limited contact spot between the rollers and deformed part significantly reduces the overall loads and provides the ability to form quite large parts from a wide range of difficult-to deform materials with a relatively a small capacity forming machine. However, this advantage can become a problem during the development of the forming technology. The small contact area and low material strain rate sensitivity typical at room temperature can generate a limited ability to control the material flow. For this reason the flow forming process appears to be very sensitive to not only the major control parameters of the process such as the speed of the mandrel, axial feed of the rollers and thickness reduction, but also to less evident ones such as the radial and axial roller offsets and their geometry.

A review of research carried out on incremental forming in the period between 1960-1980 was offered by Kalpakjian et al (1982). However, much of this work was focused on shear spinning and although this and flow forming have some similarities, the difference in the nature of deformation is quite significant, so in this paper attention will be focused only on flow forming (tube spinning). Bennich (1976) published work containing a detailed examination of the mechanics of flow forming, illustrating his analysis with physical modelling and predictions for microstructural development. This contributed much to understanding the nature of the process and helped in establishing a correlation between process parameters and loads as well as the deformation observed in the process. However, such approaches for physical modelling indirectly assume that materials with different elastic-plastic properties will behave similarly during flow forming and will have a comparable response to changes in process parameters (e.g. increasing or decreasing feed rate, thickness reduction, rollers geometry etc.). Kalpakcioglu (1964) examined the

behaviour of a number of materials (mild steels, 6xxx Al alloys, Copper) which had a yield stress in the range of 250-500 MPa and exhibited strong strain hardening. These metals provided good formability, however, it is not clear that this would be true for the High Strength Steels, Ti, Ni or Al-Li alloys, which are required in modern technological applications. Kalpakcioglu (1964) suggested an experimental procedure which might be used to assess the limits of formability. The usefulness of this approach is discussed in more detail in section 4 below.

Later research focused more on the analysis of different geometrical, kinematic and dynamic characteristics of the Flow Forming process without much discussion about how the results obtained might apply to materials with different types of elastic-plastic behaviour. The work of Ma (1993) was devoted to finding the optimal angle of attack for the tooling in tube spinning. The work of M.J. Roy et al (2015); (2010); (2009) focused on analyses of the contact between tools and workpiece and investigation of the nature of the strain distribution using finite element (FEM) simulation along with direct experimental methods.

As far as the authors are aware, the question about the influence of the elastic-plastic properties of the workpiece material was indirectly touched on in only two papers. Rajan et al. (2002) analysed the effect of the heat treatment of AISI 4130 steel on flow formability and ten years later similar work was repeated by Podder et al. (2012) for AISI 4340 steel. In both cases three heat treatments were studied: annealing, normalizing and hardening & tempering for AISI 4130; annealing, spheroidizing, hardening & tempering for AISI 4340. In the case of the 4130 steel, the authors obtained similar shapes of stress-strain curves, differing only in scale – the yield (proof stress) changed from about 400 MPa to 800 MPa, but the level of strain hardening and elongation remained the same. For 4340 the situation was different – the annealed steal had the highest strain hardening, the hardened & tempered condition the lowest. The main purpose of both papers was to find the effect of heat treatment on the final mechanical properties of formed tubes. Flow-formability was mentioned only in Podder et al (2012) and was measured in terms of three parameters: spindle load, spring-back and

geometric ovality. This is a very different vision of flow formability than that proposed by Kalpakjian et al (1982), which shows that even the definition of flow formability (or tube spinnability) is not self-evident and requires further discussion.

In order to design and optimise the process the role of the elastic-plastic properties of a material needs to be better understood. There are two pertinent aspects here. Firstly, many materials allow variation of their mechanical properties via different heat treatments. Secondary, when choosing which material to use for a part there are materials with different costs, but relatively close final properties. The designer has to consider which material or heat treatment should be preferred if flow forming is kept in mind as a manufacturing process. In Fig. 1a. it can be seen that the two martensitic precipitation-hardening stainless steels 15-5 PH® and 17-4 PH® have relatively similar mechanical properties and a wide range of possible heat treatments, but normally 15-5 PH® is costlier than 17-4 PH®. Both steels have high strength, are of interest for aerospace applications and are difficult to deform, which may make incremental bulk forming attractive. To optimise material and process choice further understanding is therefore useful.

The mechanics of flow forming are complicated. There is a combination of local loading (in the area of the tooling) and general deformation of the preform as a shell (with constraints of different types and shifting loads). This process is characterised with strongly triaxial stress states, non-monotonous loading with the possibility of cyclic changes in load from tensile to compressive and continuous changing of principal loading directions. The question then arises of which theory of plasticity and which fracture models are the most suitable for an adequate description of the process and what mechanical testing methodology is necessary and sufficient to calibrate these models? Here we start from the standard tensile properties of the material and some classical 2D (two-dimensional) models. If some clarity about the basic logic of the process can be achieved at this level, then the analysis can be expanded to more advanced levels.

As a first approach, any uniaxial tensile stress-strain diagram (or the universal equivalent stress-strain curve, if it exists) can be characterized with the following five main parameters, see Fig. 1b:

1. E – Young's modulus,
2. σ_y – yield (proof) stress,
3. Υ – normalised strain hardening/softening factor, where: $\gamma = \frac{1}{\sigma}\frac{\partial\sigma}{\partial\varepsilon}$ (in which σ is stress and ε is strain), which can be associated with the original absolute value of the tangential modulus $\gamma_0 = \frac{\partial\sigma}{\partial\varepsilon}$.
4. σ_u – ultimate stress,
5. δ – limiting tensile elongation.

Additionally, the tensile test gives us the value of ψ – the maximum area reduction.

This is what normally is known about a material before trying to optimise the process parameters. In this paper an attempt is made to understand how these parameters affect the behaviour of the material during flow forming.

a) 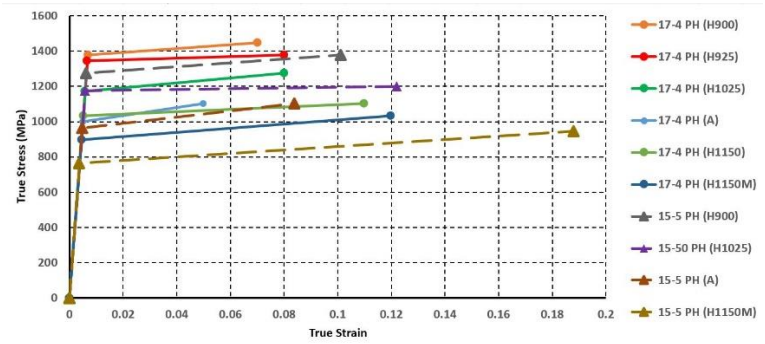

b) 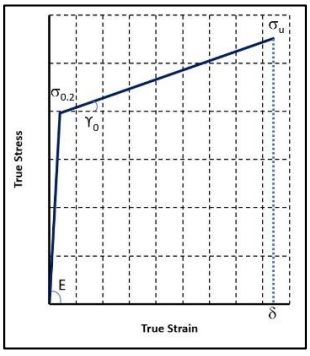

Fig. 1. a) The details of the stress-strain curves of martensitic AK steel 15-5 PH® and 17-4 PH® with typical heat treatments "15-5 PH data sheet" (2007), "17-4 PH data sheet" (2007); b) the scheme of basic elasto-plastic parameters used for formability assessment.

2. Experimental procedure and numerical simulations

The scheme of a standard flow forming setup is shown in Fig. 2a. The mandrel is directly driven and rotates at a constant rate. The workpiece (WP) is formed over the mandrel and is fixed to it on one side with the tailstock. The preform rotates together with the mandrel, though the material is free to expand or flow along the mandrel. Three rollers, located at an equal angle of 120° with each other, are free to rotate about their axis and are driven by the friction developed at the contact with the WP (hence, partial slipping is possible). These three rollers travel parallel to the axis of the shaft and converge in the radial direction to shape the required profile of the WP; the motions of the rollers are controlled using a CNC program. For the present work flow forming trials were performed with a WF STR 600-3/6 flow forming machine shown in Fig. 2b.

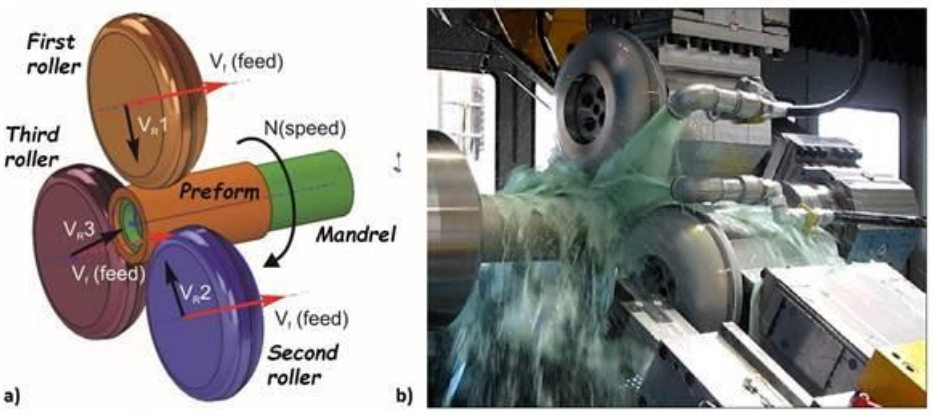

Fig. 2. a) The scheme of a standard flow forming setup; b) the Flow Former used by the authors; WF STR 600-3/6.

An FEA simulation of the flow forming operation was made using QForm metal-forming modelling software. It was assumed that material of the WP exhibited elastic-plastic isotropic hardening. It remains an open question whether isotropic hardening gives an acceptable level of simulation accuracy, or, due to a certain amount of cyclic loading in the nature of the process, some variant of the translation-hardening plastic model should be used, e.g. that described by Nouailhas et al. (1985). However, this discussion is beyond the scope of this

paper. Having as the main aim the understanding of the "logic" of the process and obtaining some general assessments, the simulation results are used here only for supportive and illustrative purposes and do not pretend to have predictive preciseness; this would require more accurate calibration and validation of the constitutive model used.

The kinematic scheme in the model of the process followed that shown in Fig. 2a. The mandrel and preform were directly driven (taking into account gravity and inertia effects). The rollers were free to rotate (with a resistance torque of about 40 Nm at the shafts), the rotation depending on the friction at the contact between the roller and preform. The only difference between the actual process and the model was the inversion of the translatory motion of the rollers. From the viewpoint of numerical convenience (mainly mesh adaptation), the mandrel with the preform was assigned a translatory motion along the axis instead of the rollers. As the feed rate in these processes was relatively low (about 2 mm/s), this inversion is not expected to make any difference to the results of the simulation.

3. Analysis of the process logic

From a practical point of view, on the basis of experience in flow forming of different materials, roughly three main categories can be distinguished: "good", "intermediate" and "poor". "Good" materials have sufficient formability for achieving large thickness reductions and elongations (sometimes up to 87% of thickness reduction and about 300% of relative elongation at room temperature) without defects. Here, thickness reduction is defined (traditionally for industrial applications) as the differential in thickness between the preform and the final flow formed part:

$$T_R = \frac{t_0 - t_f}{t_f} \cdot 100\%, \qquad \text{Eq. (1)}$$

where T_R is thickness reduction, t_0 and t_f are initial and final thickness of the walls of the tubular parts. Of course, from the viewpoint of mechanics, it would be more correct to use

logarithmic measure, e.g. $\ln\left(\frac{t_0}{t_f}\right)$, however, the industrial measure expressed by Eq.(1) will be used in this paper for the sake of simplicity of comparison with results published in the majority of cited papers. It should however, be borne in mind that this process involves a series of cycles of deformation and therefore the accumulated strain will be different to that obtained from such a simple calculation.

Materials with intermediate properties can also be flow formed, but the forming approach is not evident and is often accompanied by the formation of different surface defects. The last category contains materials that undergo fracture in the early stages of the forming process. It does not always mean that these materials cannot be formed at all, but forming them (if possible) is difficult and belongs to the category of "know-how" which is often protected by patents. It is interesting to note that many high strength materials that would not be considered readily deformable at room temperature e.g. HS steels, surprisingly fall into the category of "good" materials, while well-known ductile materials, e.g. some aluminium alloys, appear to have intermediate properties when subjected to flow forming. It might be expected that adiabatic heating would raise the forming temperatures significantly, however in practice large amounts of coolant are used in the process (see Fig.2b) so such effects can be ignored – measurements have shown that the temperature after forming does not exceed 40-50 ^{o}C.

Here, the question arises as to whether it is possible to define these formability categories more quantitatively, in some measurable units. Although, this question is very natural, and intuitively clear to any experienced engineer dealing with flow forming, even a first approach to an answer is not evident. As noted, Podder et al. (2012) have suggested three parameters as a measure of flow formability: the spindle load, spring back and ovality. These parameters may be acceptable for the comparison of a few heat treatments of the same material formed on the same machine with the same settings, as was shown in the paper cited, but hardly forms the basis for a general comparison of different materials used for flow forming of

different parts. The percentage of maximum thickness reduction per (single) pass could be considered as a candidate, as suggested in the papers of Kalpakcioglu (1964) and Kalpakjian and Rajagopal (1982) or the ratio of maximum thickness reduction to maximum elongation (or cross-sectional reduction) in tension – to distinguish between ductility and flow formability. However, these parameters still depend on the process design and do not fully express all of what is assumed in the words "good" or "intermediate". It could be suggested that these notions rather reflect the width of the process window – the range in which the process parameters can safely varied about the optimal ones.

Unfortunately, being based mainly on practical observations, this classification also does not give any *a priori* knowledge as to which category a material may be in until is it actually processed. Trials required to understand this may be quite costly and may not always deliver the required answer – sometimes failure can result from the wrong forming program rather than the material properties. In this section, a potential correlation between the characteristics of the tensile stress-strain diagram and flow formability of a material will be examined.

The logical scheme of the mechanism of flow forming for materials with "good" and "intermediate" formability is presented in Fig. 3. As is shown here, the main purpose of the flow forming process is to redistribute the original volume of the material along the mandrel. Initially, as the roller commences to deform the material, the area located under the roller compresses elastically (Fig. 3b). The higher the yield stress value, the more significant the elastic volumetric compression and a larger amount of elastic strain energy is accumulated in the deformed region. When the roller moves from this position, the load applied by it is released and the elastically compressed material tries to restore its original volume. However, it is restricted from behind and the bottom by the fixed constraints (Fig. 3c), and a plastically deformed zone is formed on the top of it. This is where strain hardening plays a crucial role. The higher the strain hardening, the bigger the difference in strength between the almost-elastic material at the bottom and the hard plastically deformed material at the outer surface. This stronger material on top restricts any upward elastic expansion (i.e. limits the spring-

back effect) and directs it towards the only free direction – along the mandrel. Thus, the material expands shifting the rest of the preform along the mandrel, and the process repeats. As a result, it is possible to achieve very large elongations due to the domination of hydrostatic pressure during the process (this point will be discussed in more detail later in the paper). An example of a flow formed part made of "good" material is shown in the Fig. 4a.

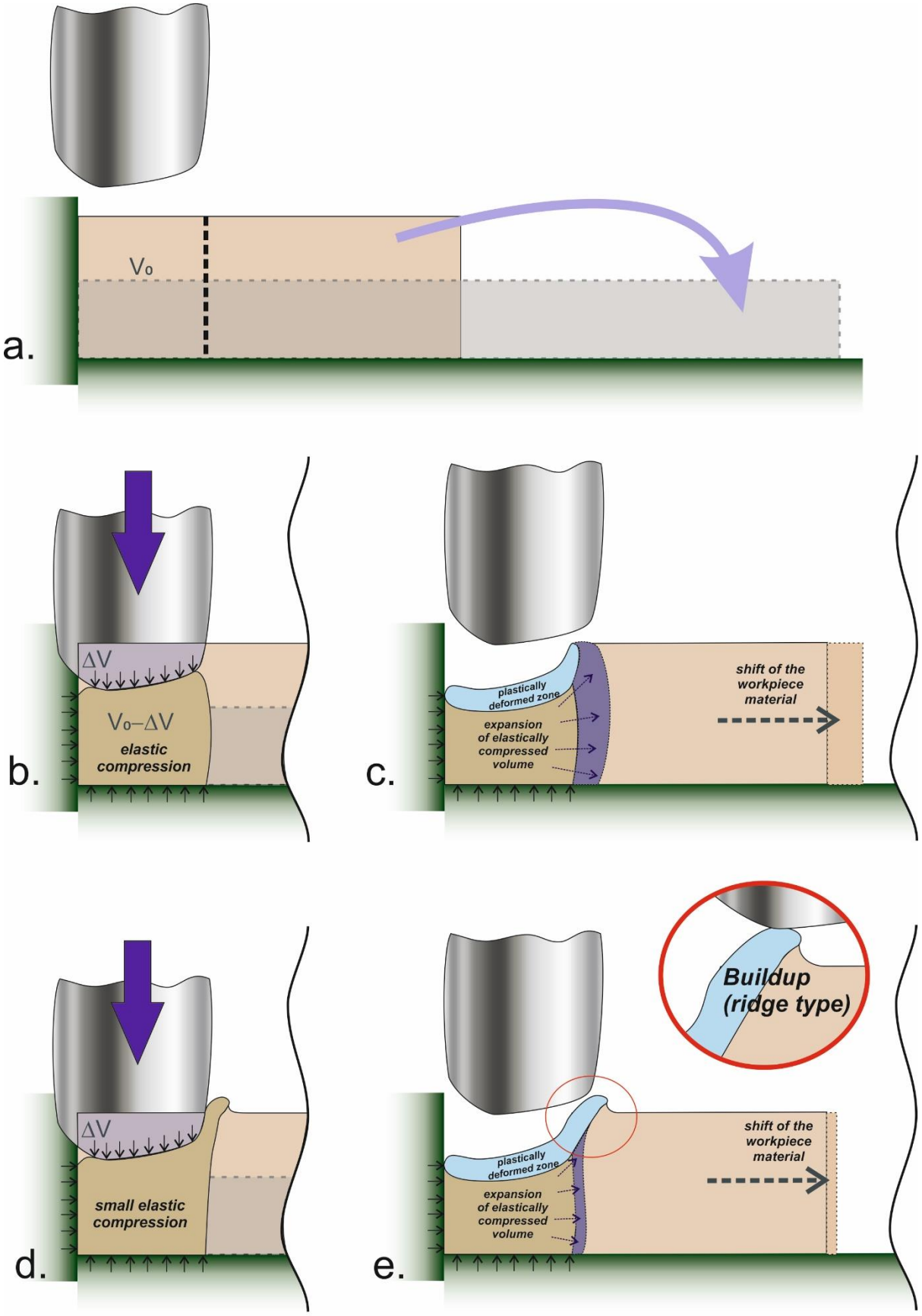

Fig. 3. Schematic of the principles of the flow forming mechanism for materials with “good” formability (a,b,c) and “intermediate” formability (a,d,e).

In the case of soft and ductile materials, the situation is different. The elastic compression of the material under the roller is reduced, because the force needed for plastic deformation of such materials is low. Therefore, instead of being elastically compressed, the material, when displaced by the roller, flows plastically towards the surface in front of the roller (Fig. 3d). To get an improved material distribution the thickness reduction in each pass must be large – 50% or more (Fig. 3e) – which can result in cracking. At the same time, as the process proceeds there is a build-up of plastically deformed material on top of the original material in front of the roller and additional problems are created. As the rollers move forward these parts of the WP tend to form flakes and chips at the contact point with the rollers; this effect is often observed during forming of aluminium parts. Such chips get stuck to the tools or get into the coolant stream and start to spoil the formed surfaces; see for example Fig. 4b. This type of problem was mentioned by Nagarajan et al. (1981) as well as discussed in the earlier works of Kalpakcioglu (1964), though those authors mainly related development of the build-up to the roller geometry and process parameters. Some authors, e.g. Gur et al. (1982) suggests to treat the build-ups (bulging up of the outer surface) as an indicator of unstable process. In this investigation, a wide range of materials were formed with the same set of the rollers and similar settings, this brought to the observation that formation of build-up depends not only on the process parameters, but also significantly depends on material properties. Even more, process settings have to be chosen depending on the material properties depending on the material properties to achieve process stability.

a. 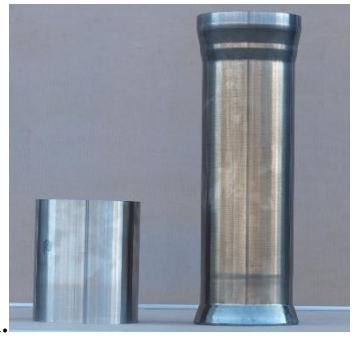 b.  c. 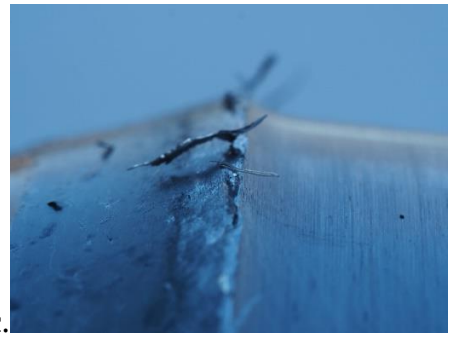

Fig. 4. An example of parts flow formed (by the authors) at room temperature from "good" and "intermediate" materials. a) "good" material – HS steel, preform and final part; b) "intermediate" material – Al6082 T4, build-up of the material ahead of the roller instead of creating longitudinal extension; c) Al6082 T4, example of chip formation in front of the rollers.

In support of the schematic shown in Fig. 3 and to gain more insight, the difference in materials' behaviour can be illustrated with the classical problem of the penetration of a rigid sphere into an elastic-plastic half-space (excluding now all the issues related to the roller geometry). The result of the simulation of this problem (axisymmetric, 25mm sphere penetrated with 2mm/s speed to the depth of 20 mm) is shown in Table 1 and illustrated schematically in Fig. 5.

Table 1. A comparison of the influence of different material properties on deformation response for a rigid sphere penetrating an elastic-plastic half-space.

Material	Steel 17-4PH H900	Artificial 1	Artificial 2	Artificial 3	Artificial 4
Material model	Elastic-plastic linear hardening	Elastic-plastic linear hardening	Rigid-plastic linear hardening	Elastic-ideal plastic (no hardening)	Elastic-plastic linear hardening
Young's Modulus, GPa	200	200	∞	200	200
Yield Stress, MPa	1380	1380	1380	1380	**690**
Ultimate Stress, MPa	1460	**2920**	1460	**1380**	**730**
Tensile ductility, δ	0.07	0.07	0.07	0.07	0.07
Modulus of Resilience, x10^6 J/m^3	4.76	4.76	**0**	4.76	**1.19**
Average hardening $\gamma_{av} = \frac{1}{\sigma_y}\frac{\sigma_u - \sigma_y}{\delta}$	0.8	**1.6**	0.8	**0**	0.8
Height of build-up, mm	1.825	-1.19	5.247	5.116	2.501
Max. depth at which $V_H \geq 0.1\ \frac{mm}{s}$, mm	56.737	57.047	35.025	44.179	49.392

To obtain the axial expansion of the flow formed material, we are mainly interested in the distribution field of the horizontal velocities in front of and under the penetrating object (sphere or roller). The deeper and more uniform this field, the more uniform the expansion of

the preform, which in turn means a more stable process and uniformity of final microstructure formation. This study clearly shows that that the main role in providing this belongs to the elastic properties of material, or, more particular to the modulus of resilience. In case of the rigid plastic material (Fig 5, third column), assuming that the resilience of material is zero, the total deformation of the material is localised around the penetrating object, little or no deformation in the vertical direction is observed. This also shows the necessity to simulate flow forming as an elastic-plastic problem as stated in Biba et al., (2015). Wider variation of the material parameters have shown that Young's modulus and yield stress separately don't have much individual importance and the Modulus of Resilience is a sufficient parameter to reflect the role of both of them.

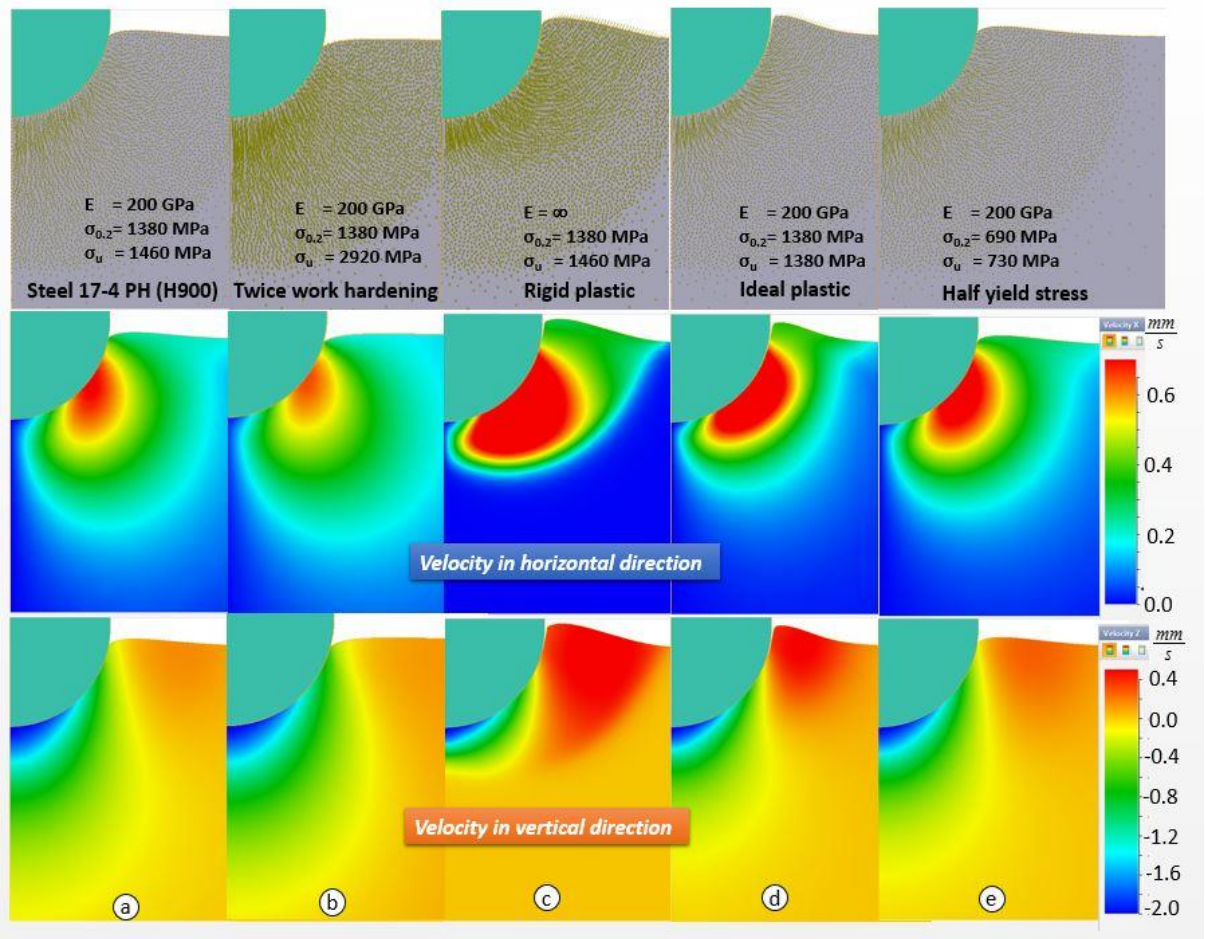

Fig. 5. The velocity field obtained in the simulation of the penetration of a rigid sphere into materials with different elasto-plastic properties: general velocity vector field $\vec{v} = \dot{x}\hat{i} + \dot{y}\hat{j}$

(first row), the field of the horizontal velocity (second row), the field of vertical velocity (third row).

To illustrate this point with regard to the effect of yield stress, Fig. 6 presents the stress-strain diagrams of two other materials; Al2099 and Ti6Al4V, which have a yield stress quite close to the steels discussed above and 8–10% elongation up to fracture, yet demonstrate fracture at an early stage of the flow forming process. It may be considered that the main reason for this early failure is low ductility. Of course, elongation to fracture as low as 8–10% does not simplify the process design; however, precipitate-hardening steel 15-5 PH in the "as received" (solution treated and air cooled) condition having the stress-strain diagram shown in Fig. 6a and a limit of only 8% tensile elongation, was nevertheless successfully flow formed with a thickness reduction from 15 mm to 3.5 mm (about 77%). This means that, with respect to the flow formability of these materials, the key difference between the elastic-plastic properties is likely to be the strain hardening level; Υ.

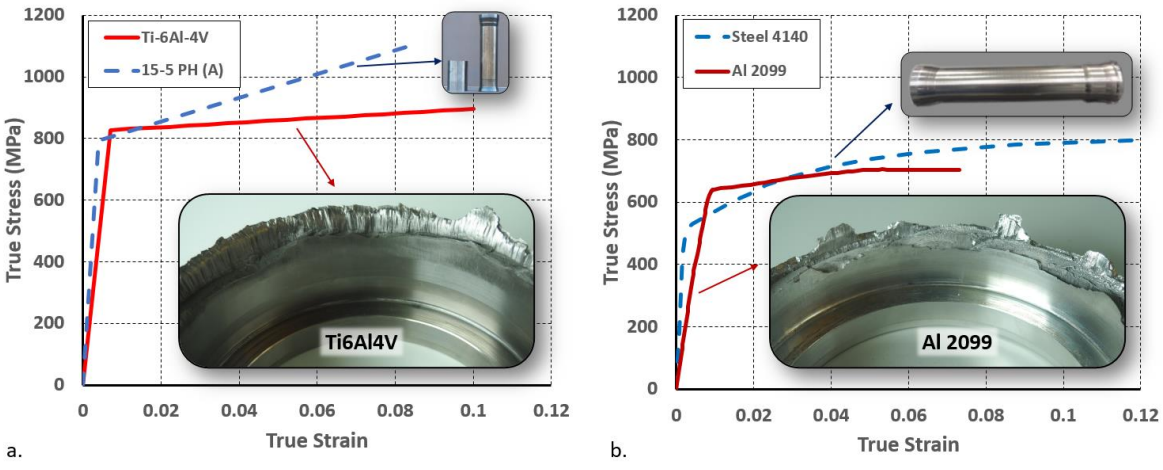

Fig. 6. Stress-strain diagrams and fractured preforms of "poor" or "difficult to flow form" materials: a) Ti6Al4V, b) Al2099.

It can be also seen from the Table 1 and Fig 5 that strain hardening does not much affect the depth of material flow, but significantly affects to the amount of build-up (and correspondingly the stability of the process). Strain hardening higher than 1 completely

removes positive build up (see Fig.5 column 2). However, unfortunately it hardly explains why high strain hardening prevents the formation of chevron cracks, which produced early failure of the materials shown in Fig.6.

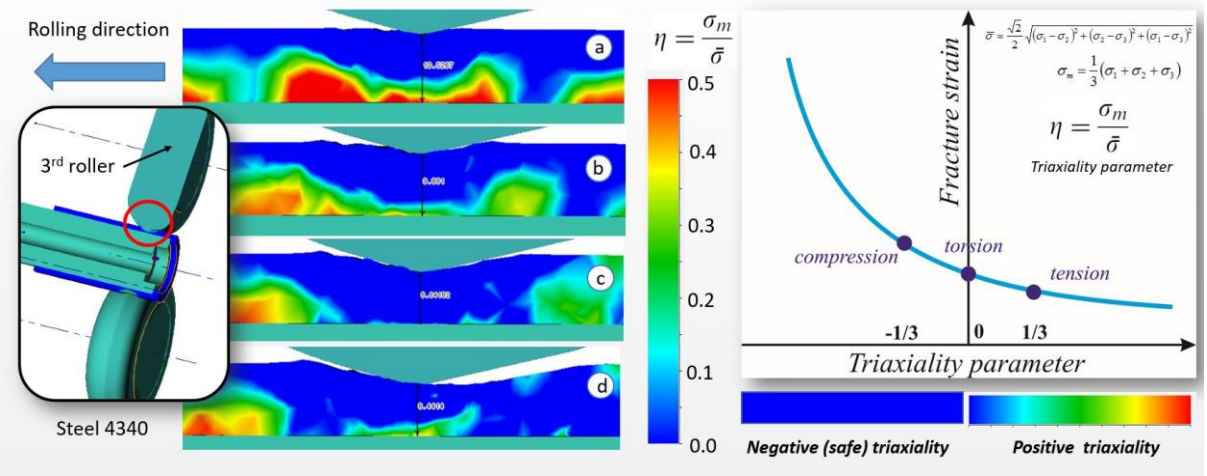

Fig. 7. A map of the positive triaxiality in the workpiece during different stages of flow forming, i.e. thickness reduction: a) 11.5→10.5mm, b) 11.5→10.5, c) 11.5→9.9, d) 11.5→8.2. Material Steel 4340 SPH, Modulus of Resilience; 1.12 x10^6 J/m^3, the strain hardening is shown in the Fig.10. The scale has been chosen to highlight the positive (i.e. tensile and thus potentially dangerous) triaxiality states – all negative (compressive) triaxiality is blue.

To understand the role of strain hardening, it is worth analysing how the flow forming process can provide the ability to deform the material considerably beyond its tensile limit.

One of the most evident reasons, well known in metal forming, is the link between fracture and the triaxiality state. A generic schematic of the triaxiality state in the preform during the flow forming process obtained from FEA simulation is shown in Fig. 7. Here it should be noted that we use the general engineering terms ‘compressive’ and ‘tensile’ with respect to negative and positive triaxiality to reflect the general nature of the stress state. However, it is appreciated that from a pure mechanics point of view these states are in fact more complex than pure tension or compression. Having said this, it can be seen that the process provides compressive hydrostatics (i.e. the mean stress or the first invariant of the stress tensor is

negative) directly under the roller. Fracture in this area is unlikely. Dangerous positive (tensile) hydrostatics are significant in the initial stages of penetration (this has a low dependence on material strain hardening). They are then gradually replaced with a safer distribution of compressive hydrostatics providing optimal conditions for the deforming of the materials with low ductility. At a later stage of the process positive triaxiality again appears at the bottom of the formed part, reflecting the presence of the axial tensile force produced by the rollers moving ahead against the material.

Hence, the spot in front of the roller is safe – there is no deformation. The location under and slightly ahead of the roller is more vulnerable to fracture, and as can be seen in Fig. 8a, chevron cracking can be initiated in that location (similar effects were noted in Kalpakjian et al (1982)). However, as can be observed from Fig. 8e, the amount of accumulated plastic deformation at this location is quite small and the axial component of the strain tensor is much smaller than the limiting tensile elongation; about 0.04 true strain (n.b. that the loading has a cyclic nature so the accumulated plastic deformation is higher than the equivalent von-Mises strain). This though does not give an answer as to why the crack was initiated. The nature of the fracture surface, shown in Fig. 8b and Fig. 8c for both Ti6Al4V and Al2099, shows that the initial stage of fracture was almost purely brittle; ductile fracture occurring only when the brittle crack reached the plastically deformed zone (red in Fig. 8e.). This suggests that it was the stress that was critical for the crack initiation. In Fig. 8d, a small zone of tensile stress (normal stress in the axial direction) can be seen. Whether this amount of stress is sufficient to cause fracture requires further analysis (most probably it is an interplay between crack initiation and crack development in the field of large residual stresses – the inverse side of a large resilience). It would therefore appear when a material exhibits a high level of strain hardening local tensile stresses can be accommodated (to some degree at least). If the strain hardening is insufficient any stress concentrator can become critical for the initiation of a brittle crack, which then actively develops under the large residual stresses that are formed after the passage of the rollers (see Fig. 3).

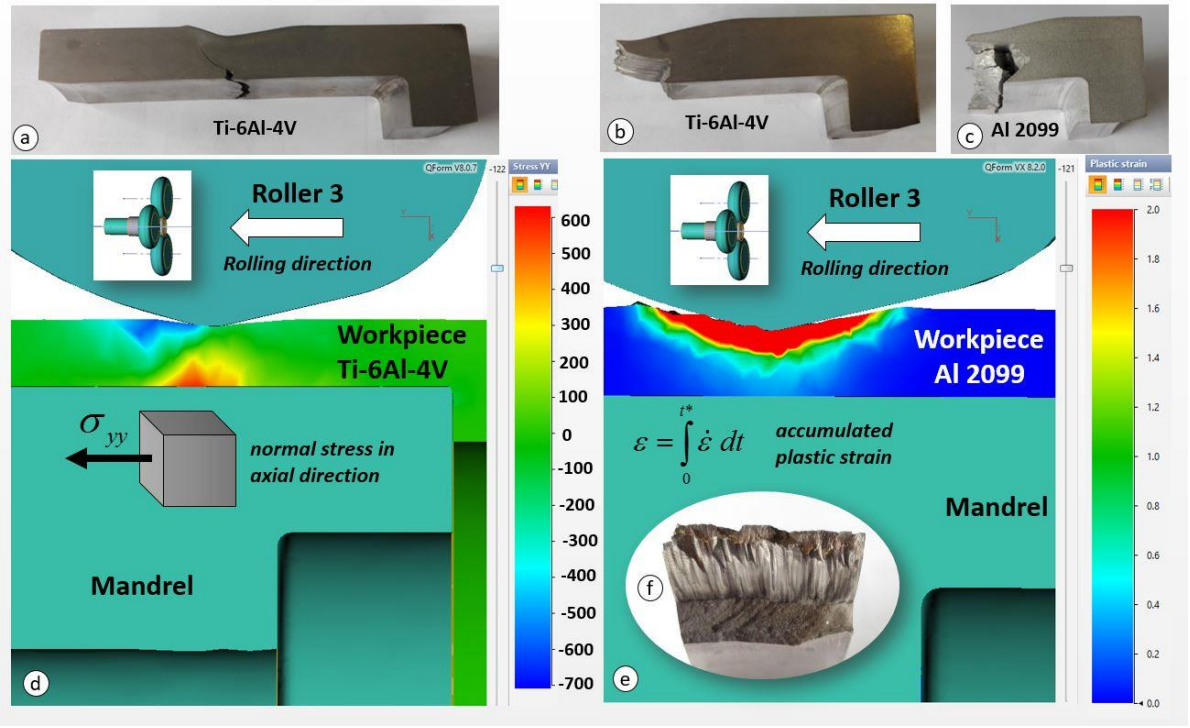

Fig. 8. Chevron cracking and fracture observed during flow forming of a. & b.) Ti6Al4V, c) Al2099; d) map of the normal component of the stress tensor in the direction of rolling, e) map of the accumulated plastic deformation Al2099, f) typical fracture surface for this type of failure. Note that d) and e) show deformation of only the third roller - in practice more than one roller is used; as shown in Fig. 2b three rollers are operative with the second and third following the first so that the level of deformation progressively increases (not shown here).

4. Flow formability (spinnability) test

Kalpakcioglu (1964) proposed a special experimental method for assessing the flow formability of tubes (which he termed spinnability). The purpose of this was to find the maximum possible reduction of tube thickness per *single* spinning pass. The scheme of this test is shown in Fig. 9a. The roller moves along the mandrel and penetrates into the material at an angle, φ. The aim of the test is to find the limit after which the material breaks in tension behind the roller. This, no doubt, is a very important test for finding the limiting depth of roller penetration in a single path, but does not necessarily demonstrate the limits of

flow formability (as the author himself mentions in the discussion). As discussed by the author and additionally proven by the damage evaluation made recently by Ma et al. (2015), the triaxiality state at which fracture takes place in this test is very close to that of pure tension. Besides this, the large gradient in thickness between the thinnest region and the remaining part of the preform develops a case of localised deformation reminiscent of necking in tension. So, it is not surprising that the forming limits obtained are in good correlation with the maximum area reduction measured from tensile tests (though the question of the possibility of a quantitative correlation is still not clear). However, the total idea of flow forming and its basic approach (offering a large deformation for materials with limited ductility) is to avoid this situation. As per the nature of the flow forming process, the action of the tools should create in the zone of active deformation a state with dominating hydrostatic compressive pressure (large negative values of triaxiality factor), which significantly increases the effective fracture strain. The incremental character of the process in its turn tends to oppose the development of strain localisation (by creating a sort of floating neck) – the material is deformed locally in one place, then the roller moves and the next region is deformed slightly more while the recently deformed area is somewhat unloaded. As may be inferred from the illustration in Fig. 9a, in this spinnability test, even though it formally remains incremental, as the "step" in front of the roller becomes bigger, the axial pressure exerted by the roller(s) on the unformed part of workpiece transforms into tensile force around the entire circumference of the tubular part. This is clearly visible in the results of the modelling reported in Ma et al. (2015).

To take into account all the benefits of flow forming, and to establish the general limits of flow formability (not per single reduction), an alternative test is proposed by the authors (see schematic shown in Fig. 9b). This test consists of several successive passes. In each pass, the thickness is reduced by some optimal amount (typically 20%). Each time the rollers move along the complete length of the preform each progression being started with an axial shift forming a series of steps. Of course, in comparison with the previous test, the latter test takes

more passes to complete, but this is the cost for an attempt to have a similar level of triaxiality at all stages of deformation.

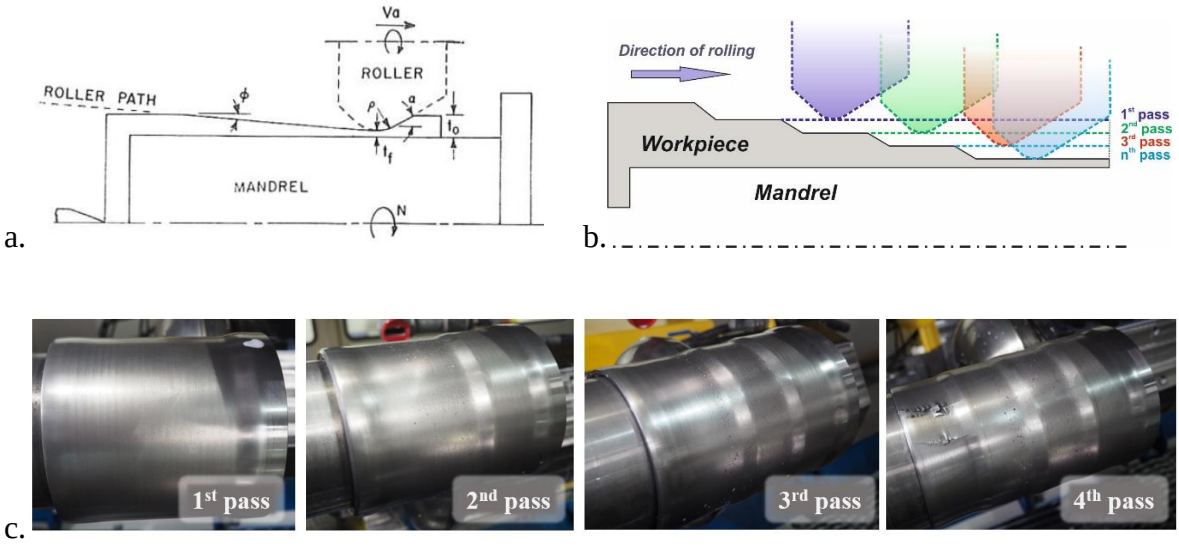

Fig. 9. The spinnability test a) as proposed by Kalpakcioglu (1964) and Kalpakjian and Rajagopal (1982); b) a proposed alternative test and c) experimental results from trials carried out by the authors (15-5 PH HT1150 steel).

In principle, these two tests may be considered to complement each other. The spinnability test of Kalpakcioglu (1964) can be taken as a lower bound assessment, whereas that shown in Fig. 9b would form the upper bound. This suggestion can be illustrated with the following example. Two spinnability tests were carried out to understand the potential of 17-7PH steel with H900 heat treatment (which significantly increases the strength but reduces the ductility of material). The spinnability "cone" test of Kalpakcioglu produced fracture following a thickness reduction from 15 to 8.7mm. However the "step" test allowed a final thickness of 2.9 mm to be achieved without fracture (further reduction was technically difficult with our equipment). This outcome depends on the thickness reduction on each pass (it remains an open question what is general spinnability). But from the practical point of view this result is very useful, because it helps to establish the reduction strategy suitable for the particular material. Once obtained in the "step" test a maximum reduction is stably repeatable in real forming with different geometries.

It should be noted however that although both tests can serve the purpose of assessing the flow formability or spinnability of the material, they remain as qualitative trials rather than a full test suitable for standardisation. Unfortunately, in both cases, the limits obtained besides depending on the mechanical properties of the material, are also strongly influenced by the process parameters and geometry. This is why the question of finding a correlation between the ***standard*** elastic-plastic characteristics of a material and its flow-formability remains important.

5. Results and Discussion

With respect to the above mentioned hypothesis, assumptions and examples, the following summary can be drawn: the problem of the assessment of flow-formability of materials demands -

a. the formulation of a stricter and more scientific definition of what we understand as "flow formability" and to decide some numerical measures for grading it;
b. to find a correlation between the elastic-plastic characteristics of material behaviour (under complex loading; typical of flow forming) and the level of its flow formability

To distinguish between common plastic ductility and flow-formability, two main aspects have to be taken into account in defining flow-formability. The first aspect is how suitable is a material for flow-forming – to what degree do its characteristics match the main mechanics of this process and how wide a process window does it provide? A measure of this can be the percentage of deviation of the process parameters about the optimal ones without the loss of flow stability within the process, i.e. limited changes in the process control parameters (feed, speed, depth of penetration per path, rollers' geometry and offsets) result in continuous, smooth and predictable changes in output characteristics (thickness reduction, surface quality, etc.). As was discussed and illustrated in Fig. 3 and Fig. 4, the dominating physical principle utilized for the longitudinal spread of the material is elastic resilience – the elastic energy of the material compressed under the roller is transferred into the work of pushing as yet un-

deformed material along the mandrel. This suggests that materials with a higher level of resilience should give more freedom in designing the process, and this can possibly be further developed into a numerical correlation between the material resilience and level of flow-formability.

Another elastic-plastic characteristic of the material which extends or shrinks the process window is of course the fracture limit. However, as was shown with the example of Ti6Al4V or Al 2099, the tensile limit (δ) is most probably not the best characteristic to estimate it. As shown in Fig. 6a, a material with a lesser tensile elongation can exhibit superior flow formability and even a relatively limited tensile elongation may not be a big obstacle for flow forming. As was previously mentioned, Kalpakcioglu, (1964) reported that the tensile reduction of area, ψ, has a better correlation with spinnability (in his definition of it). One of his conclusions stated that "for materials with a tensile reduction of area above 45% a maximum reduction in spinning of about 80% is the limit, irrespective of ductility. For materials below 45%, spinnability will depend on their ductility." This is a very valuable conclusion, but there are two circumstances forcing us to look for some additional measures. As was discussed in Section 4, Kalpakcioglu examined only materials with quite similar strain hardening and in his tests assumed the limiting spinnability as correlating to the instant when the material undergoes failure in tension behind the roller. If we are talking about modern flow forming processes, especially spinning with several rollers, when all process optimization is focused on the homogeneity of deformation and the minimisation of strain localisation, then tension in the formed portion of the preform rarely appears to be the source of damage or failure.

This draws attention to another parameter, historically related with the stability of metal flow; strain hardening: $\gamma = \frac{1}{\sigma}\frac{\partial\sigma}{\partial\varepsilon}$. Our forming experience shows that this parameter is very important and maybe even is the key material characteristic for the flow forming process. It is intuitively clear why this parameter affects the process window. At room temperature, when

the thermal and stain rate sensitivity of the material is very limited, work hardening remains almost the only available control measure against localisation of deformation and brittle fracture. As per the classical criteria of flow localisation developed by Hart and Ghosh (1977), the beginning of flow localisation for uniaxial tension directly depends on the instantaneous hardening value. Assuming that strain rate sensitivity is negligible at room temperature (i.e. m≈0) and taking the suggestion of Ghosh (1977) that deformation is considered to be stable as long as it is accompanied by a load rise, even though imperfections in a specimen may be growing, we get the following relationship:

$$\delta P = \sigma \delta A + A \delta \sigma \geq 0 \qquad \text{Eq. (2)}$$

Substituting into equation (22) the following: $\delta\sigma = \sigma \cdot \gamma \delta\varepsilon$, and $\varepsilon = -\ln\left(\frac{A}{A_0}\right)$, where A and A_0 are the instantaneous and initial cross-sectional area of the tensile specimen, respectively, we obtain:

$$\delta P = \sigma \delta A + A \cdot \sigma \cdot \gamma \cdot \left(-\frac{\delta A}{A} + \frac{\delta A_0}{A_0} \right) \geq 0$$

$$\gamma \geq \left[\frac{1}{1 - \frac{\delta \ln A_0}{\delta \ln A}} \right] \qquad \text{Eq. (3)}$$

Although all these equations are derived for uniaxial tension and can hardly be directly applied to the case of complex loading observed during flow forming, an attempt can nevertheless be made to use them for initial screening. Fig. 10 shows the evolution of strain hardening during deformation for the different materials mentioned in this paper.

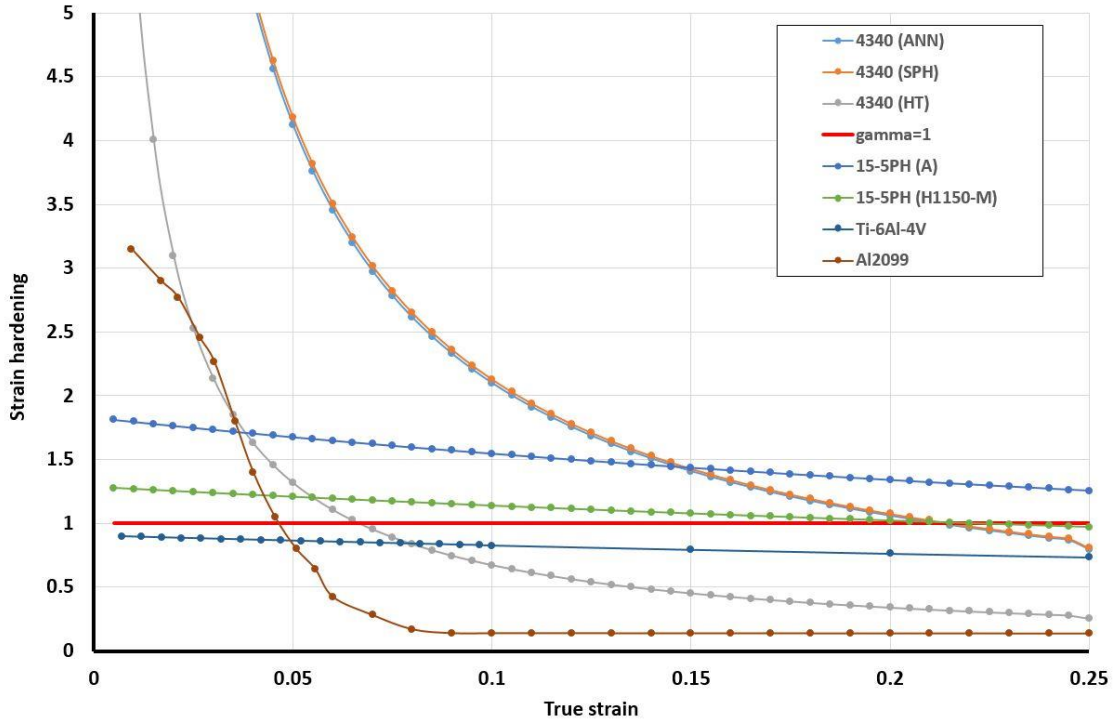

Fig. 10. The value of the instantaneous strain hardening (ϒ) for different materials.

Two materials with low strain hardening: Ti6Al4V (with ϒ<1), and Al2099 (where ϒ drops below 1 quite rapidly), have demonstrated cracking at the very beginning of flow forming (see Fig. 6, Fig. 7). To establish some numerical thresholds, it is useful to analyse hardened and tempered AISI4340, reported by Podder et al. (2012). Having quite high strain hardening at the beginning of deformation, this material demonstrates fast degradation of hardening, which reduces below 1 as early as 0.07 in true strain. As per the observation of Podder et al. (2012), a preform with this heat treatment was successfully flow formed in two passes up to a resultant 71% of thickness reduction with no defects observed. However, it should be noted that the flow forming described in Podder et al. (2012) was of a reversed type (i.e. the material moves in the opposite direction to the tool travel), which means that the direct tensile load on the formed part is excluded and only bending stresses would be likely to generate cracking. This raises an additional question, whether the flow-formability of the material is different for direct and reverse flow forming. It seems that the principles of deformation

shown in Fig. 3 will remain almost the same, while the conditions causing fracture may be different.

While ϒ characterises instantaneous strain hardening and is different at different stages of loading, another parameter also related with the total amount of strain hardening was used in Kalpakcioglu, (1964):

$$k = \frac{\int_0^{\varepsilon_f} \sigma \cdot d\varepsilon}{\sigma_f \cdot \varepsilon_f} \qquad \text{Eq. (4)}$$

Here, ε_f and σ_f are the strain and stress at fracture correspondingly, for an ideal plastic material, k=1, and for any hardening material k<1. The bigger the difference between yield and ultimate stress, the smaller the value of k. As is clear from equation (4), k is relatively independent of the value of the limiting strain and, correspondingly, on the gradients of the true stress- true strain curve – this is the main difference between k and ϒ. As per available experience, ϒ looks to be a more suitable parameter, reflecting both the dynamics of strain hardening as well as the instantaneous state, although it is not yet clear how to establish a quantitative relationship between its values and flow formability. Regarding k, some suggestions on the dependence of maximum thickness reduction in spinning on this parameter was suggested in Kalpakcioglu (1964) (though this is a very rough relation based on many assumptions, simplifying the triaxiality state, neglecting friction, etc.):

$$Max\ thickness\ reduction = 1 - e^{-1/k} \qquad \text{Eq. (5)}$$

This equation, however, does not look very promising. For an ideal plastic material with k=1, the maximum thickness reduction will be 63%, and hence, any hardening material must have at least that amount of safe reduction. At the same time, the experimental trials showed that, for example, Al2099 having k≈0.9 failed at less than 20% of thickness reduction during flow forming.

In summary, it may be reiterated that developing predictive measures for flow formability is a complex issue. It involves a variety of challenges: all-component strain and stress trajectories, changes in geometry and location of the yield surface, non-symmetrical loading and unloading. It is simplistic to suppose that there is a chance to understand and describe the total history of such a significantly non-uniaxial and continuously changing plastic deformation with data generated by simple uniaxial tension. However, tensile data is almost the only information about a material that is normally available in an industrial environment before defining the process parameters (and before performing initial process modelling as well). That is why it is so important to understand how to interpret this data correctly and what set of advanced material properties is required as the next step of process optimisation.

6. Conclusions

1. It has been shown that the mechanics of plastic deformation within the flow forming process is complex and characterised by:

a) a significantly non-uniaxial and non-uniform stress-strain state with a possibility of high gradients of stress and strain,
b) a continuous change of the location of the zone of active plastic deformation, which leads to the development of low cycle non-symmetric loading
c) the appearance of fracture which is dependent on a combination of factors including:
   - the fast development of small defects assisted within the field of the tensile residual stresses, which are formed as an unavoidable part of forming process,
   - the triaxiality state and,
   - any propensity for flow localisation should the flow become unstable

2. The complexity of the process leaves little opportunity to develop a full understanding using only standard uniaxial tensile data. However, given that this is often the only data easily available some guidance on how to relate these properties to the nature of the flow

forming process is offered in this paper. In addition, a new material evaluation procedure is proposed that when used with the approach outlined by Kalpakcioglu (1964) offers a more thorough evaluation of the flow formability of prospective alloys.

3. Three uniaxial elastic-plastic characteristics of a material seem to be the most important for flow forming processes: resilience, strain hardening and tensile area reduction. They influence flow-formability (or tube spinnability) of the material, although this notion itself can be understood and numerically characterised in several different ways.

Acknowledgement:

The authors would like to offers thanks to Messier-Bugatti-Dowty & Prof. Trevor Dean for useful inputs and the rotary processes team at the AFRC for the experimental trials.

Funding: This work was supported by the HVM Catapult, UK.

References

AK Steel 15-5 PH stainless steel data sheet, 2007 [http://www.aksteel.com]

AK Steel 17-4 PH stainless steel data sheet, 2007 [http://www.aksteel.com]

Bennich, P., 1976. Tube spinning. Int. J. Prod. Res. 14, 11–21.

Biba, N., Vlasov, A., Stebunov, S., Maximov, A.E., 2015. An Approach to Simulation of Flow Forming Using Elastic-Visco-Plastic Material Model, in: 13th INTERNATIONAL COLD FORMING CONGRESS, GLASGOW.

Ghosh, A., 1977. Tensile instability and necking in materials with strain hardening and strain-rate hardening. Acta Metall. 25, 1413–1424.

Gour M., and Tirosh J., 1982 Plastic Flow instability under compressive loading during shear spinning Processes. J. Eng. Ind. 104, 17-22.

Kalpakcioglu, S., 1964. Maximum Reduction in Power Spinning of Tubes. J. Eng. Ind. 86, 49-51.

Kalpakjian, S., Rajagopal, S., 1982. Spinning of tubes: A review. J. Appl. Metalwork. 2, 211–223.

Ma, H., Xu, W., Jin, B.C., Shan, D., Nutt, S.R., 2015. Damage evaluation in tube spinnability test with ductile fracture criteria. Int. J. Mech. Sci. 100, 99–111.

Ma, Z.E., 1993. Optimal angle of attack in tube spinning. J. Mat. Proc. Tech. 37, 217–224.

Mohebbi, M.S., Akbarzadeh, A., 2010. Experimental study and FEM analysis of redundant strains in flow forming of tubes. J. Mat. Proc. Tech. 210, 389–395.

Nagarajan, H.N., Kotrappa, H., Mallanna, C., Venkatesh, V.C., 1981. Mechanics of Flow Forming. CIRP Ann. - Manuf. Technol. 30, 159–162.

Nouailhas, D., Chaboche, J.L., Savalle, S., Cailletaud, G., 1985. On the constitutive equations

for cyclic plasticity under nonproportional loading. Int. J. Plast. 1, 317–330.

Plewinski, A., Denger, T., 2009. Spinning and flow forming hard-to-deform metal alloys. Arch. Civ. Mech. Eng. 9, 101–109.

Podder, B., Mondal, C., Ramesh Kumar, K., Yadav, D.R., 2012. Effect of preform heat treatment on the flow formability and mechanical properties of AISI4340 steel. Mater. Des. 37, 174–181.

Rajan, K.., Deshpande, P.., Narasimhan, K., 2002. Effect of heat treatment of preform on the mechanical properties of flow formed AISI 4130 Steel Tubes—a theoretical and experimental assessment. J. Mat. Proc. Tech. vol. 125-126, 503–511.

Roy, M.J., Klassen, R.J., Wood, J.T., 2009. Evolution of plastic strain during a flow forming process. J. Mat. Proc. Tech. 209, 1018–1025.

Roy, M.J., Maijer, D.M., 2015. Analysis and modelling of a rotary forming process for cast aluminum alloy A356. J. Mat. Proc Tech. 226, 118-204.

Roy, M.J., Maijer, D.M., Klassen, R.J., Wood, J.T., Schost, E., 2010. Analytical solution of the tooling/workpiece contact interface shape during a flow forming operation, J. Mat. Proc. Tech 210, 14, 1976-1985.

Figure captions

Fig. 11. a) The details of the stress-strain curves of martensitic AK steel 15-5 PH® and 17-4 PH® with typical heat treatments "15-5 PH data sheet" (2007), "17-4 PH data sheet" (2007); b) the scheme of basic elasto-plastic parameters used for formability assessment.

Fig. 12. a) The scheme of a standard flow forming setup; b) the Flow Former used by the authors; WF STR 600-3/6.

Fig. 13. Schematic of the principles of the flow forming mechanism for materials with "good" formability (a,b,c) and "intermediate" formability (a,d,e).

Fig. 14. An example of parts flow formed (by the authors) at room temperature from "good" and "intermediate" materials. a) "good" material – HS steel, preform and final part; b) "intermediate" material – Al6082 T4, build-up of the material ahead of the roller instead of creating longitudinal extension; c) Al6082 T4, example of chip formation in front of the rollers.

Fig. 15. The velocity field obtained in the simulation of the penetration of a rigid sphere into materials with different elasto-plastic properties: general velocity vector field $\vec{v} = \dot{x}\hat{i} + \dot{y}\hat{j}$ (first row), the field of the horizontal velocity (second row), the field of vertical velocity (third row).

Fig. 16. Stress-strain diagrams and fractured preforms of "poor" or "difficult to flow form" materials: a) Ti6Al4V, b) Al2099.

Fig. 17. A map of the positive triaxiality in the workpiece during different stages of flow forming, i.e. thickness reduction: a) 11.5→10.5mm, b) 11.5→10.5, c) 11.5→9.9, d) 11.5→8.2. Material Steel 4340 SPH, Modulus of Resilience; 1.12 x10^6 J/m^3, the strain hardening is shown in the Fig.10. The scale has been chosen to highlight the positive (i.e. tensile and thus potentially dangerous) triaxiality states – all negative (compressive) triaxiality is blue.

Fig. 18. Chevron cracking and fracture observed during flow forming of a. & b.) Ti6Al4V, c) Al2099; d) map of the normal component of the stress tensor in the direction of rolling, e) map of the accumulated plastic deformation Al2099, f) typical fracture surface for this type of failure. Note that d) and e) show deformation of only the third roller - in practice more than one roller is used; as shown in Fig. 2b three rollers are operative with the second and third following the first so that the level of deformation progressively increases (not shown here).

Fig. 19. The spinnability test a) as proposed by Kalpakcioglu (1964) and Kalpakjian and Rajagopal (1982); b) a proposed alternative test and c) experimental results from trials carried out by the authors (15-5 PH HT1150 steel).

Fig. 20. The value of the instantaneous strain hardening (ϒ) for different materials.

Table caption

Table 1. A comparison of the influence of different material properties on deformation response for a rigid sphere penetrating an elastic-plastic half-space.